

PAPER • OPEN ACCESS

Non-perturbative QCD and hadron physics

To cite this article: J J Cobos-Martínez 2016 *J. Phys.: Conf. Ser.* **761** 012036

View the [article online](#) for updates and enhancements.

Related content

- [Hadrons in AdS/QCD models](#)
Henrique Boschi-Filho
- [Non-perturbative QCD Effect on K-Factor of Drell–Yan Process](#)
Hou Zhao-Yu, Zhi Hai-Su and Chen Jun-Xiao
- [The leading non-perturbative coefficient in the weak-coupling expansion of hot QCD pressure](#)
F. Di Renzo, M. Laine, V. Miccio et al.

Non-perturbative QCD and hadron physics

J J Cobos-Martínez

Instituto de Física y Matemáticas, Universidad Michoacana de San Nicolás de Hidalgo,
Edificio C-3, Ciudad Universitaria, Morelia, Michoacán 58040, México.

E-mail: j.j.cobos.martinez@gmail.com

Abstract.

A brief exposition of contemporary non-perturbative methods based on the Schwinger-Dyson (SDE) and Bethe-Salpeter equations (BSE) of Quantum Chromodynamics (QCD) and their application to hadron physics is given. These equations provide a non-perturbative continuum formulation of QCD and are a powerful and promising tool for the study of hadron physics. Results on some properties of hadrons based on this approach, with particular attention to the pion distribution amplitude, elastic, and transition electromagnetic form factors, and their comparison to experimental data are presented.

1. Introduction

The quantitative understanding of the properties of strongly interacting matter in all its manifestations and forms in terms of the fundamental theory, Quantum Chromodynamics, is without a doubt one of the most challenging and exciting problems in modern science [1, 2, 3, 4, 5, 6, 7]. QCD is the fundamental theory of quarks, gluons, and their interactions. However, the QCD Lagrangian does not by itself explain the data on strongly interacting matter, and it is not clear how the observed bound states, the hadrons, and their properties arise from QCD. Neither confinement nor dynamical chiral symmetry breaking (DCSB) is apparent in QCD's lagrangian, yet they play a dominant role in determining the observable characteristics of QCD. The physics of strongly interacting matter is governed by emergent phenomena such as these, which can only be elucidated through the use of non-perturbative methods in QCD [4, 5, 6, 7]

The SDE-BSE are a well suited continuum approach to non-perturbative QCD and hadron physics [5, 6, 7] since they provide access to infrared as well as ultraviolet momenta, thus giving a clear connection with processes that are well understood because QCD is asymptotically free. The SDE-BSE form an infinite tower of coupled non-linear integral equations that must be truncated in order to define a tractable problem. Because QCD is asymptotically free the interaction kernel in each SDE is known within the perturbative domain and hence any model dependence is restricted to the long-range behavior of the kernels. The SDE-BSE connect observables with QCD's fields and parameters, and feedback between theory and experiment can then refine the statements and lead to an understanding of non-perturbative QCD and hadron physics. The mass spectrum of hadrons, hadron elastic and transition form factors, distribution functions, and the phase structure of hot and dense QCD, all contribute information that is critical to elucidate the non-perturbative interaction between quarks and gluons. Existing and future hadron physics laboratories around the world will be accumulating data so that for the first time we will be able to see the transition from non-perturbative physics (mesons and baryons)



to the perturbative domain (quarks and gluons), governed by QCD. Providing predictions that can be tested experimentally is very important. An understanding of the emergent phenomena of confinement and DCSB from first principles will surely provide us the foundations for an understanding of hadron physics from QCD.

2. Electromagnetic structure of hadrons and pQCD predictions

The investigation of matter's substructure through electron scattering experiments is a well-proved technique since the electromagnetic (EM) probe is well known. Suppose that we want to study the EM charge distribution of a hadron, for example the pion of Fig 1. The experimental procedure is to measure the angular distribution of the scattered electrons and compare it to the known cross section for scattering electrons from a point charge

$$\frac{d\sigma}{d\Omega} = \left(\frac{d\sigma}{d\Omega} \right)_{\text{point}} |F(q^2)|^2, \quad (1)$$

where $q = k' - k = P' - P$ is the momentum transfer carried by the virtual photon and $F(q^2)$ is the hadron's EM form factor (FF). We then attempt to deduce the structure (and dynamics of its constituents) of the target from the measured FF. The amplitude for the Feynman diagram

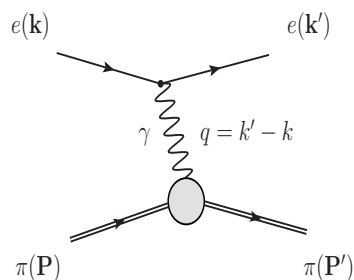


Figure 1. Electron-pion scattering.

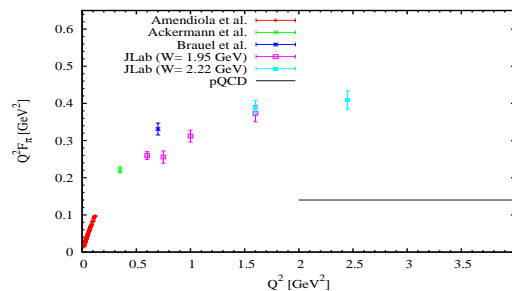


Figure 2. $F_\pi(Q^2)$ and pQCD prediction.

of Fig 1 is given by

$$\mathcal{M} = (-ie)^2 \bar{u}(k') \gamma^\mu u(k) \frac{-i}{q^2} \langle \pi(P') | J_\mu | \pi(P) \rangle, \quad (2)$$

where u , \bar{u} are electron spinors, $|\pi(P)\rangle$ is the full pion bound state, and J_μ its EM current. The quantity $\langle \pi(P') | J_\mu | \pi(P) \rangle$ is the pion-photon vertex, whose structure we do not know and would like to understand in terms of the non-perturbative interactions between quarks, gluons, and photons, from their underlying theories. Although we do not know the details about $\langle \pi(P') | J_\mu | \pi(P) \rangle$ in terms of QCD and QED dynamics, we know that J_μ must be a Lorentz four-vector, and therefore the EM interaction of a spinless particle, like the pion, can be parametrized by a single FF

$$\langle \pi(P') | J_\mu | \pi(P) \rangle = (P' + P)_\mu F_\pi(Q^2), \quad (3)$$

where $F_\pi(Q^2)$ is the pion FF that appears in Eq. (1) and we have defined $Q^2 \equiv -q^2$ since q^2 is negative for electron scattering. The FF parametrizes our ignorance about the detailed structure of the pion and the dynamics of its substructure, represented by the blob in Fig 1. In principle, it can be calculated from perturbative QCD (pQCD) for large Q^2 because QCD is asymptotically free. However, it is not clear whether presently accessible momentum transfers are large enough to test predictions based on a perturbative analysis in QCD. For low-to-present-day momentum transfers, the contributions coming from the dynamics of strong QCD play an important, if

non-dominant, role. In this regime, pQCD is inapplicable and other methods that incorporate these effects must be developed.

According to Brodsky and Lepage [8, 9], the large Q^2 limit of lepton-hadron scattering processes can be factorized into a soft part containing the non-perturbative long-range dynamics, absorbed into a universal distribution amplitude (DA), and a hard scattering amplitude T_H , which encodes the quark-gluon subprocesses and can be calculated in pQCD, for the high-momentum exchange between the lepton and the valence quarks in the hadron. Thus $F_\pi(Q^2)$ can be written as [8, 9]

$$F_\pi(Q^2) = \iint dx dy \phi_\pi^*(x, Q^2) T_H(x, y; Q^2) \phi_\pi(y, Q^2), \quad (4)$$

where $\phi_\pi(x, Q^2)$ is the pion DA (PDA) and x (y) is the fraction of the pion momentum P (P') carried by the individual valence quarks, $0 < x, y < 1$. The hard scattering kernel is a sum over contributions from one-gluon exchange, two-gluon exchange, and so on. Due to the asymptotic freedom of QCD, in the $Q^2 \rightarrow \infty$ limit Eq. (4) is dominated by one-gluon exchange [8, 9]. Thus

$$F_\pi(Q^2) \stackrel{Q^2 \rightarrow \infty}{\simeq} 16\pi \frac{\alpha_s(Q^2)}{Q^2} \left| \frac{1}{3} \int dx \frac{1}{x} \phi_\pi(x) \right|^2, \quad (5)$$

where α_s is QCD's coupling constant, and xyQ^2 is the ‘‘virtuality’’ of the exchanged gluon, which sets the scale for $\alpha_s(Q^2)$ and can be understood as a measure of the applicability of pQCD to the interaction. In the $Q^2 \rightarrow \infty$ limit the PDA evolves to [8, 9] $\phi_\pi^{\text{asy}}(x)$

$$\phi_\pi(x, Q^2) \stackrel{Q^2 \rightarrow \infty}{\longrightarrow} \phi_\pi^{\text{asy}}(x) = 6f_\pi x(1-x), \quad (6)$$

where $f_\pi = 92.2$ MeV is the pion decay constant. Using Equations (5) and (6) one gets the pQCD prediction [8, 9] for $F_\pi(Q^2)$

$$\lim_{Q^2 \rightarrow \infty} Q^2 F_\pi(Q^2) = 16\pi f_\pi^2 \alpha_s(Q^2). \quad (7)$$

Brodsky and Lepage [8, 9] have also provided pQCD predictions for the transition FF $G_{\pi^0\gamma\gamma^*}(Q^2)$ that parametrizes the process $\gamma\gamma^* \rightarrow \pi^0$

$$\lim_{Q^2 \rightarrow \infty} Q^2 G_{\pi^0\gamma\gamma^*}(Q^2) = 4\pi^2 \frac{1}{3} \int dx \frac{1}{x} \phi_\pi(x, Q^2) = 4\pi^2 f_\pi, \quad (8)$$

where we have used the asymptotic form of $\phi_\pi(x, Q^2)$. Note that in the both pQCD predictions for $F_\pi(Q^2)$ and $G_{\pi^0\gamma\gamma^*}(Q^2)$, the quantity $\frac{1}{3} \int dx \frac{1}{x} \phi_\pi(x, Q^2)$, or the universal PDA $\phi_\pi(x, Q^2)$, controls their normalization. The PDA plays an important role in the theoretical description of many QCD processes [10]. Equations (7) and (8) are just two examples. The PDA also plays a role in semileptonic weak decays $B \rightarrow \pi l \nu$ and weak hadronic decays $B \rightarrow \pi\pi$, both of which contribute to the determination of the parameters of the quark mixing matrix in the Standard Model; see, for example, Ref. [10]. The precise definition of $\phi_\pi(x, Q^2)$ is based on the representation as the matrix element of a non-local quark-antiquark operator on the light-cone formalism; its x -dependence cannot be computed from pQCD but its evolution with Q^2 can.

The experimental measurement of $F_\pi(Q^2)$ is a non-trivial task. To date, reliable experimental data for $F_\pi(Q^2)$ exist in the timelike (negative Q^2) region, for small spacelike values of Q^2 , where $F_\pi(Q^2)$ is dominated by the ρ meson pole, and up to $Q^2 = 2.45$ GeV²; see, for example, Ref. [11]. We are awaiting JLAB's 12 GeV upgrade to extend the above measurements up to $Q^2 = 6$ GeV². In Fig 2 the pQCD prediction for $F_\pi(Q^2)$ is compared to the available experimental data. As can

be seen, for the highest Q^2 data available, there is a weak suggestion that $Q^2 F_\pi(Q^2) = \text{constant}$ is being approached. Since these data are several times larger than the pQCD prediction, non-perturbative effects are still dominant. A question that comes to mind is: Has $\phi_\pi(x, Q^2)$ reached its asymptotic value $\phi_\pi^{\text{asy}}(x)$ at present energies? For a comparison of the experimental data on $G_{\pi^0\gamma\gamma^*}(Q^2)$ to the pQCD prediction and recent SDE results, see Khépani Raya's contribution to these conference proceedings and also Ref. [12].

3. The Schwinger-Dyson equations

The Schwinger-Dyson equations are the equations of motion for the Greens functions of a quantum field theory (QFT). These are derived from the full generating functional of the theory, making no assumptions about the coupling constant. In the Euclidean space formulation of QCD, the renormalized SDE for the full quark propagator, see Fig 3, for a particular quark flavor is

$$S^{-1}(p) = Z_2 i\gamma \cdot p + Z_4 m(\mu) + Z_1 \int \frac{d^4q}{(2\pi)^4} g^2 D_{\mu\nu}(p-q) \frac{\lambda^a}{2} \gamma^\mu S(q) \Gamma^{a\nu}(p, q), \quad (9)$$

where g is QCD's coupling constant, $D_{\mu\nu}$ is the gluon propagator, $\Gamma^{a\nu}$ is the quark-gluon vertex, and $m(\mu)$ the renormalized current-quark mass; $Z_1(\mu, \Lambda)$ and $Z_2(\mu, \Lambda)$ are renormalization constants, which depend on the renormalization (μ) and regularization (Λ) mass scales. The quark propagator, the gluon propagator, and the quark-gluon vertex, also depend on μ ; however observables do not. Both $D_{\mu\nu}$ and $\Gamma^{a\nu}$ satisfy their own SDE, which in turn are coupled to higher n -point functions and so on *ad infinitum*. Thus the quark SDE, explicitly shows that the SDEs form a coupled infinite set of non-linear integral equations. A tractable problem is defined once a truncation scheme has been specified. See, for example, Refs. [5, 6, 7] for more details on SDEs and their application to non-perturbative QCD and hadron physics. The general form

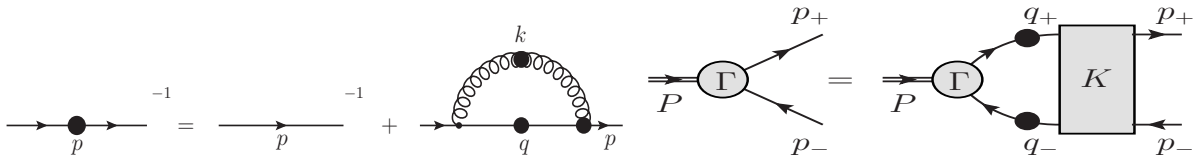


Figure 3. Quark Schwinger-Dyson equation **Figure 4.** Meson Bethe-Salpeter equation

of the quark propagator is given in terms of two Lorentz-scalar dressing functions

$$S^{-1}(p) = i\gamma \cdot p A(p^2, \mu^2) + B(p^2, \mu^2) = Z^{-1}(p^2, \mu^2) (i\gamma \cdot p + M(p^2)). \quad (10)$$

In the last form, $Z(p^2, \mu^2)$ is known as the wave function renormalization and $M(p^2)$ is the quark mass function. The solution of Eq. (9) is further subject to a renormalization condition [7]. The best known truncation scheme of the SDEs is the weak coupling expansion. It is an essential tool for the investigation of large momentum transfer phenomena because QCD is asymptotically free. However, it excludes the possibility of obtaining information about the low-energy regime of the strong interactions [5, 6, 7]. As an example of this, consider the chiral limit in pQCD. In this case the theory is chirally symmetric and a perturbative evaluation [13, 14] gives

$$B(p^2) = m[1 - (\alpha/\pi) \ln(p^2/m^2) + \dots], \quad (11)$$

where the ellipsis denote higher order terms in α . However, it is always true that at any order in pQCD $\lim_{m \rightarrow 0} B(p^2) = 0$ and hence DCSB is impossible in perturbation theory.

4. The Bethe-Salpeter equation

Meson bound states, whose flavor structure is given by a dressed quark-antiquark pair, are described by the Bethe-Salpeter equation (BSE), see Fig 4,

$$[\Gamma_H(p; P)]_{tu} = \int \frac{d^4q}{(2\pi)^4} [K(p, q; P)]_{tu;rs} \left[S^a(q_+) \Gamma_H(q; P) S^b(q_-) \right]_{sr}, \quad (12)$$

where $H = (a\bar{b})$ indicates the flavor structure; $\Gamma_H(p; P)$ is the meson Bethe-Salpeter amplitude (BSA) describing the bound state; $S^f(q_\pm)$ is the quark propagator, obtained from Eq. (9); $K(p, q; P)$ is the quark-antiquark scattering kernel; Latin indices indicate the color, flavor, and Dirac structure; Poincaré covariance and momentum conservation entail $q_+ = q + \eta P$, $q_- = q - (1 - \eta)P$, etc, with $P = p_+ - p_-$. The parameter $\eta \in [0, 1]$ describes the meson's momentum (P) sharing between the quark-antiquark pair; observables, however, do not depend on this. The BSE is a homogeneous eigenvalue equation that admits solutions only for discrete values of the meson momenta $P^2 = -m_H^2$, where m_H is the meson mass [5, 6, 7]. In a particular channel, the lowest mass solution corresponds to the ground state. In the pseudoscalar channel the lowest mass solutions are the pion and kaon mesons. The general form of the BSA in this channel is given by

$$\Gamma_H(p; P) = \gamma_5 [iE_H(p; P) + \gamma \cdot P F_H(p; P) + \gamma \cdot p (p \cdot P) G_H(p; P) + \sigma^{\mu\nu} p_\mu P_\nu H_H(p; P)]. \quad (13)$$

Since the BSE is homogeneous, the BSA has to be normalized by a separate condition [5, 6, 7]. For a more detailed presentation of the SDE-BSE and their application to hadron physics see, for example, Refs [5, 6, 7]. In Eq. (12), $K(p, q; P)$ is the fully-amputated, two-particle irreducible, quark-antiquark scattering kernel. It is a four-point Schwinger function, obtained formally as the sum of a countable infinity of skeleton diagrams. The complexity of $K(p, q; P)$ is one of the reasons why quantitative SDE-BSE studies employ modeling of $D_{\mu\nu}$ and $\Gamma^{a\nu}$, because $K(p, q; P)$ also appears in the SDE satisfied by $\Gamma^{a\nu}$. Despite their complexity, substantial progress has been made in unraveling the non-perturbative structure of $D_{\mu\nu}$ and $\Gamma^{a\nu}$ using their SDE [15, 16], as well as the lattice formulation of QCD [17, 18]. Ultimately, the detailed infrared behavior of these quantities should not materially affect the observable consequences of the quark SDE and meson BSE, as long as the infrared enhancement in the quark SDE implements the appropriate amount of dynamical chiral symmetry breaking and, explains the (pseudo)Goldstone character of the pion [5, 6, 7]. However, the lack of a full understanding of the interaction between quarks, through the complete knowledge of $K(p, q; P)$, does not prevent us from obtaining general results in hadron physics [19].

5. The rainbow-ladder truncation and the Maris-Tandy model

In QCD, chiral symmetry and its breaking pattern are the dominant effects in the low-energy regime, specially for light quarks. These are expressed through the axial-vector Ward-Takahashi identity (AxWTI) [19, 20, 21], which implies a relationship between the kernel in the BSE and that in the quark SDE (through the quark self-energy $\Sigma(k)$)

$$\int \frac{d^4q}{(2\pi)^4} K_{tu;rs}(k, q; P) [\gamma_5 S(q_-) + S(q_+) \gamma_5]_{sr} = [\Sigma(k_+) \gamma_5 + \gamma_5 \Sigma(k_-)]_{tu}, \quad (14)$$

thus constraining the content of $K(p, q; P)$ if an essential symmetry and its breaking pattern are to be preserved. This relation must be satisfied by any viable truncation scheme of the SDE-BSE coupled system. In modeling the quark SDE kernel we follow [20, 21], and make use of the rainbow approximation for the self-energy

$$Z_1 \int \frac{d^4q}{(2\pi)^4} g^2 D^{\mu\nu}(k) \frac{\lambda^a}{2} \gamma_\mu S(q) \Gamma^{a\nu}(k, p) \rightarrow \int \frac{d^4q}{(2\pi)^4} \mathcal{G}(k^2) D^{\text{free}\mu\nu}(k) \frac{\lambda^a}{2} \gamma_\mu S(q) \frac{\lambda^a}{2} \gamma_\nu, \quad (15)$$

where the phenomenological “effective” coupling $\mathcal{G}(k^2)$ contains information about the product $G(k^2, \mu^2)F^1(k, p, \mu)$, where $F^1(k, p, \mu)$ is the form factor associated with the γ_ν structure in the quark-gluon vertex and $G(k^2, \mu^2)$ that in the gluon propagator. From a practical point of view Eq. (14) provides a way of obtaining $K(p, q; P)$. Equations (14) and (15) give

$$K(p, q; P)_{tu;rs} = -\mathcal{G}(k^2)D^{\text{free}\mu\nu}(k) \left[\frac{\lambda^a}{2} \gamma_\mu \right]_{ts} \left[\frac{\lambda^a}{2} \gamma_\nu \right]_{ru}, \quad (16)$$

which define the rainbow-ladder (RL) truncation of the SDE-BSE complex. Constraints on $\mathcal{G}(k^2)$ come from the SDE satisfied by gluon propagator and the quark-gluon vertex. However, we know the behavior of $\alpha(k^2)$ in the ultraviolet, $k^2 > 2\text{-}3 \text{ GeV}^2$, is well described by pQCD, and therefore any model dependence on $\mathcal{G}(k^2)$ is restricted to the infrared. On the other hand, $\mathcal{G}(k^2)$ in the quark SDE should exhibit sufficient infrared enhancement capable of triggering DCSB and the generation of a momentum-dependent quark mass dressing function that connects the current-quark mass to a constituent-like quark mass [5, 6, 7]. Various models for the effective interaction $\mathcal{G}(k^2)$ combining the ultraviolet behavior known from pQCD and an ansatz for the infrared part have been designed in the past and have been applied to different detailed studies of hadron physics; see, for example, Refs. [5, 6, 7]. In choosing a form for $\mathcal{G}(k^2)$ we use the Maris-Tandy model [20, 21]. In Fig 5 we present numerical solutions for $M(p^2)$ for various

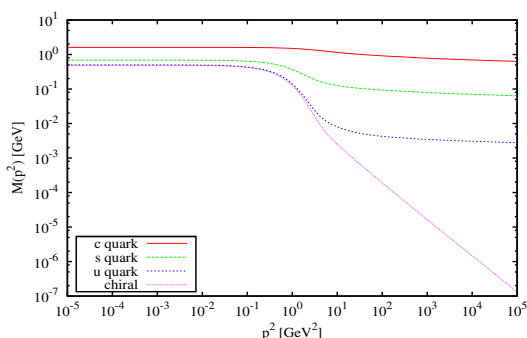


Figure 5. $M(p^2)$ in the RL truncation with the Maris-Tandy dressing function for various values of $m(\mu)$.

values of $m(\mu)$. It is evident that DCSB occurs in the rainbow truncation. At ultraviolet momenta, the magnitude of $M(p^2)$ is determined from $m(\mu)$. In the infrared, however, and specially for light-quarks, $M(p^2)$ is significantly enhanced. For light quarks, this enhancement is orders of magnitude larger than the mass present in the Lagrangian. The domain in which the effect of DCSB is relevant decreases as the $m(\mu)$ increases. We also note that the evolution from the current-quark mass to a constituent-like quark mass occurs at the scale of $\approx 1 \text{ GeV}^2$, as required from hadron phenomenology [22]. The behavior of $M(p^2)$ in Fig 5 has also been confirmed semi-quantitatively in lattice simulations of QCD [23, 24, 25].

6. SDE-BSE results on the PDA and form factors

The theoretical interest in the distribution amplitude (DA) of hadrons is due to their relevance in the description of exclusive reactions [8, 9, 26, 27] from QCD. The DAs describe probability amplitudes to find a hadron in a state with minimum number of Fock constituents and at small transverse separation. The scale dependence of the DA is given by the Efremov-Radyushkin–Brodsky-Lepage (ERBL) evolution equations [8, 9, 26] and can be calculated in pQCD, while the DA at a certain low scale provides the necessary non-perturbative input for the QCD treatment of exclusive reactions. In terms of quark propagators S and the pion BSA Γ_π , the pion DA is given by [28]

$$f_\pi \phi_\pi(x) = Z_2 N_c \text{Tr} \int \frac{d^4 q}{(2\pi)^4} \delta(n \cdot q_+ - xn \cdot P) \gamma_5 \gamma \cdot n S(q_+) \Gamma_\pi(q; P) S(q_-). \quad (17)$$

Due to the appearance of δ in Eq. (17) it is easier to calculate the integer moments of $\phi_\pi(x)$, $\langle x^m \rangle = \int_0^1 dx x^m \phi_\pi(x)$ [28]. For the computation of moments, using Feynman integral techniques and a subsequent numerical integration over the Feynman parameters introduced, algebraic parametrizations of the RL numerical solutions for S and Γ_π are employed [28]. Once all needed moments are calculated, a novel reconstruction procedure is implemented to obtain the PDA [28]. Here, the PDA is expanded in terms of Gegenbauer polynomials of order α , instead with $\alpha = 3/2$ fixed. With $\alpha_- = \alpha - 1/2$ we write

$$\phi_\pi(x, \mu) = x^{\alpha_-} (1-x)^{\alpha_-} \left[1 + \sum_{j=2,4,\dots} a_j^\alpha(\mu) C_j^\alpha(2x-1) \right]. \quad (18)$$

The parameter α and expansion coefficients $a_j^\alpha(\mu)$ are determined from the numerical moments obtained from Eq. (17). Once these are obtained one may project out the result onto an $\alpha = 3/2$ basis. However, this requires many nonzero coefficients $\{a_j^{3/2}\}$, and introduce spurious oscillations typical of Fourier-like approximations. The plot in Fig 6 shows the RL result with

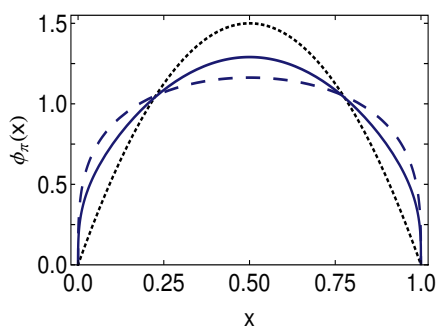


Figure 6. Computed distribution amplitude at $\mu = 2$ GeV. Curves: dashed, rainbow-ladder; and dotted asymptotic distribution.

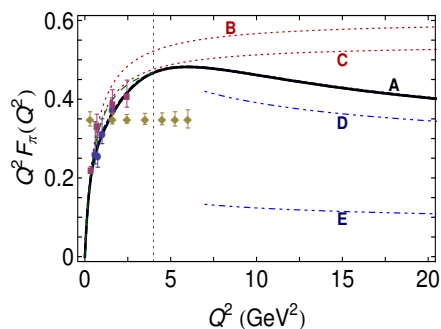


Figure 7. $Q^2 F_\pi(Q^2)$. Curves: A, prediction from Ref. [29]; D, asymptotic result using the PDA from Ref. [28]; E is the pQCD result. See Ref. [29] for more details.

the Maris-Tandy interaction [28]. It is described with $\alpha^{\text{RL}} = 0.79$, and $a_2^{\alpha^{\text{RL}}} = 0.0029$. Projected onto a $\alpha = 3/2$ basis this corresponds to $a_2^{3/2} = 0.23, \dots, a_{14}^{3/2} = 0.022$, etc; see Ref. [28] for more details on the computation and the conclusions drawn. Recall the quantity $|\frac{1}{3} \int dx \frac{1}{x} \phi_\pi(x)|^2$. The Gegenbauer expansion coefficients evolve with scale according to ERBL equations [8, 9, 26]. At leading-log accuracy it is necessary to evolve to $\mu = 100$ GeV before $a_2^{3/2}$ falls to 50% of its value [29]. This means that the asymptotic value $\phi_\pi^{\text{asy}}(x)$ lies at very large momenta. Furthermore using the asymptotic form for $\phi_\pi(x)$ we have $|\frac{1}{3} \int dx \frac{1}{x} \phi_\pi^{\text{asy}}(x)|^2 = 1$. On the other hand, using the RL result for $\phi_\pi(x)$ we have $|\frac{1}{3} \int dx \frac{1}{x} \phi_\pi^{\text{RL}}(x)|^2 = 3.2$. This means that the pQCD analysis result has to be multiplied by a factor of 3.2 and the asymptotic analysis of various models has to be compared to this new result [29], since the asymptotic domain given by pQCD lies indeed at very large momenta, far beyond our experimental capabilities; see curve E in Fig 7. Curve A in Fig 7 shows the $F_\pi(Q^2)$ computed in the RL truncation of the SDE-BSE system [29]. The magnitude of $Q^2 F_\pi(Q^2)$ reflects the scale of dynamical chiral symmetry breaking. The analysis in Ref. [29] in shows that hard contributions to the pion form factor dominate for $Q^2 \geq 8$ GeV.

7. Conclusions

The SDE-BSE is a well founded continuum approach to non-perturbative QCD and hadron physics. They are a natural framework for the exploration of strong QCD since they provide access to infrared as well as ultraviolet momenta, thus giving a clear connection with processes that are well understood because QCD is asymptotically free.

ϕ_π^{asy} is a poor approximation to $\phi_\pi(x)$ at all momentum-transfer scales that are either now accessible to experiments involving pion elastic or transition form processes, or will become so in the foreseeable future. Predictions for leading-order, leading-twist formulae involving ϕ_π^{asy} are a misleading guide to interpreting and understanding contemporary experiments. At accessible energy scales a better guide is obtained by using the PDA described herein in such formulae [12, 28, 29, 30].

References

- [1] Brodsky S J *et al.* 2015 QCD and Hadron Physics *Preprint* arXiv:1502.05728 [hep-ph]
- [2] Heinz U *et al.* 2015 Exploring the properties of the phases of QCD matter-research opportunities and priorities for the next decade *Preprint* arXiv:1501.06477 [nucl-th].
- [3] Alkofer R and von Smekal L (2001) *Phys. Rept.* **353**, 281
- [4] Brambilla N *et al.* (2014) *Eur. Phys. J. C* **74**, no. 10, 2981
- [5] A. Bashir, L. Chang, I. C. Cloet, B. El-Bennich, Y. X. Liu, C. D. Roberts and P. C. Tandy, (2012) *Commun. Theor. Phys.* **58**, 79 (2012)
- [6] I. C. Cloet and C. D. Roberts (2014) *Prog. Part. Nucl. Phys.* **77**, 1
- [7] C. D. Roberts (2016) *J. Phys. Conf. Ser.* **706**, 022003
- [8] Lepage G P and Brodsky S J 1979 *Phys. Lett B* **87** 359
- [9] Lepage G P and Brodsky S J 1980 *Phys. Rev. D* **22** 2157
- [10] V. M. Braun, S. Collins, M. Gckeler, P. Prez-Rubio, A. Schfer, R. W. Schiel and A. Sternbeck *Phys. Rev. D* **92** 014504
- [11] Cobos-Martinez J J (2010) *Static and dynamic properties of the pion from continuum modelling of strong QCD* Online: <http://theses.dur.ac.uk/633/>
- [12] K. Raya, L. Chang, A. Bashir, J. J. Cobos-Martinez, L. X. Gutierrez-Guerrero, C. D. Roberts and P. C. Tandy, *Phys. Rev. D* **93** 074017
- [13] Pagels H 1979 *Phys. Rev. D* **19** 3080
- [14] Cornwall J M 1982 *Phys. Rev. D* **26** 1453
- [15] Alkofer R, Fischer C S Llanes-Estrada F J and Schwenzer K 2009 *Annals Phys.* **324** 106
- [16] Fischer C S 2003 *Non-perturbative propagators, running coupling and dynamical mass generation in ghost - antighost symmetric gauges in QCD* *Preprint* arxiv:hep-ph/0304233
- [17] Skullerud J, Bowman P O, Kizilersu A, Leinweber D B and Williams A G 2005 *Nucl. Phys. Proc. Suppl.* **141** 244
- [18] Cucchieri A and Mendes T 2007 *PoS LAT2007* 297
- [19] Maris P, Roberts C D and Tandy P C 1998 *Phys.Lett. B* **420** 267
- [20] Maris P and Roberts C D 1997 *Phys. Rev. C* **56** 3369
- [21] Maris P and Tandy P C 1999 *Phys. Rev. C* **60** 055214
- [22] Roberts C D 2016 Perspective on the origin of hadron masses *Preprint* arXiv:1606.03909 [nucl-th]
- [23] Skullerud J, Leinweber D B and Williams A G 2001 *Phys. Rev. D* **64** 074508
- [24] Bowman P O, Heller U M, Leinweber D B and Williams A G 2003 *Nucl. Phys. Proc. Suppl* **119** 323
- [25] Bowman P O, Heller U M, Leinweber D B, Williams A G and Zhang J 2004 *Nucl. Phys. Proc. Suppl.* **128** 23
- [26] Efremov A V and Radyushkin A V 1980 *Phys. Lett. B* **94** 245
- [27] Farrar G R and Jackson D R 1979 *Phys. Rev. Lett.* **43** 246
- [28] Chang L, Cloet I C, Cobos-Martinez J J, Roberts C D, Schmidt S M and Tandy P C 2013 *Phys.Rev.Lett.* **110** 132001
- [29] Chang L, Cloet I C, Roberts C D, Schmidt S M and Tandy P C 2013 *Phys.Rev.Lett.* **111** 141802
- [30] Cloet I C, Chang L, Roberts C D, Schmidt S M and Tandy P C 2013 *Phys.Rev.Lett.* **111** 092001